Atmos. Chem. Phys. Discuss., 6, 12179–12197, 2006
www.atmos-chem-phys-discuss.net/6/12179/2006/

Atmospheric Chemistry and Physics Discussions

Is aerosol formation in cirrus clouds possible?

J. Kazil[1], E. R. Lovejoy[1], E. J. Jensen[2], and D. R. Hanson[3]

[1]NOAA Earth System Research Laboratory, Boulder, CO, USA
[2]NASA Ames Research Center, Moffett Field, CA, USA
[3]Augsburg College, Minneapolis, MN, USA

Received: 18 October 2006 – Accepted: 21 November 2006 – Published: 28 November 2006

Correspondence to: J. Kazil (jan.kazil@noaa.gov)

Abstract

The recent observation of ultrafine aerosol particles in cirrus clouds has raised the question whether aerosol formation within cirrus clouds is possible, and if so, what mechanisms are involved. We have developed an aerosol parcel model of neutral and charged H_2SO_4/H_2O aerosol processes, including nucleation from the gas phase and loss onto cirrus ice particles. Laboratory thermodynamic data for sulfuric acid uptake and loss by small neutral and charged clusters are used, allowing for a reliable description of both neutral and charged nucleation down to the very low temperatures occurring in the upper troposphere and lower stratosphere. The model implements a first order scheme for resolving the aerosol size distribution within its geometric size sections, which efficiently suppresses numerical diffusion. We operate the model offline on trajectories generated with a detailed 1-D cirrus model which describes ice crystal nucleation, deposition growth, vertical advection of ice crystals and water vapor, and ice crystal sedimentation. In this paper we explore the possibility of aerosol formation within non-convective cirrus clouds and draw conclusions for aerosol formation in anvil cirrus. We find that sulfate aerosol formation within cirrus clouds can proceed even at high ice surface area concentrations, and depends strongly on the size of the cirrus ice crystals and on the surface area concentration of preexisting aerosol particles.

1 Introduction

Aerosol formation from the gas phase requires sufficient condensable gas concentrations to permit the formation of supercritical molecular clusters which grow faster than they decay. This nucleation process is more likely to occur when preexisting aerosol surface area concentrations are low, as preexisting aerosol is a sink for condensable gases and suppresses nucleation. Preexisting aerosol also removes freshly nucleated particles by coagulation. The observation of high ultrafine aerosol concentrations in cirrus clouds by Lee et al. (2004) and the possibility that these particles formed within the cloud thus challenge conventional wisdom, as cirrus clouds typically exhibit large surface area concentrations. It has therefore been suggested that the observed ultrafine particles were artifacts of ice crystals shattering in the measurement device (Lee et al., 2004). On the other hand, the upper troposphere exhibits favorable conditions for aerosol formation, including low temperatures, and within cirrus clouds, high relative humidities. Elevated water vapor concentrations within cirrus clouds could result in an enhanced production of the hydroxyl radical and consequently of gas phase sulfuric acid. Other processes potentially promoting aerosol formation in cirrus clouds include yet unidentified heterogeneous processes on ice surfaces producing aerosol precursors, and the homogeneous nucleation of hydrophobic organic molecules (Kulmala et al., 2006).

Whether aerosol formation within cirrus clouds is possible, and if so, what mechanisms are involved is not a purely academic question: Visible cirrus cover ∼20–40% of the globe (Liou, 1986; Wang et al., 1996; Wylie and Menzel, 1999). At the same time the upper troposphere, where cirrus clouds are commonly found, is a potentially important source of new particles supplying the troposphere and stratosphere with condensation nuclei (Brock et al., 1995; Clarke et al., 1998; Eichkorn et al., 2002; Lee et al., 2003; Kazil et al., 2006). A role of cirrus in upper tropospheric aerosol formation could therefore have significant implications for tropospheric and stratospheric processes.

2 Model

We have developed an aerosol parcel model describing neutral and charged H_2SO_4/H_2O aerosol, its formation from the gas phase, and its loss onto cirrus ice crystals. The present version of the model utilizes a new treatment of the neutral H_2SO_4/H_2O cluster thermodynamic data. The hydrated H_2SO_4 dimer $(H_2SO_4)_2(H_2O)_x$ and trimer $(H_2SO_4)_3(H_2O)_y$ formation thermodynamic data, averaged over the cluster water contents, are calculated explicitly based on fits to the recent laboratory measurements by Hanson and Lovejoy (2006). These fits read, with RH over water in %,

$$dS(\text{kcal mol}^{-1}\ \text{K}^{-1}) = -0.04$$
$$dH(\text{kcal mol}^{-1}) = -18.32 - 4.55 \cdot 10^{-3} \cdot \text{RH} \quad (1)$$

for the dimer formation and

$$dS(\text{kcal mol}^{-1}\ \text{K}^{-1}) = -0.045$$
$$dH(\text{kcal mol}^{-1}) = -21.41 - 2.63 \cdot 10^{-2} \cdot \text{RH} \quad (2)$$

for the trimer formation. For the uptake and loss of sulfuric acid and water by small charged clusters the model employs laboratory thermodynamic data measured by Froyd and Lovejoy (2003b). The thermodynamic data for large aerosol particles derive from H_2SO_4 and H_2O vapor pressures over bulk solutions calculated with the Aerosol Inorganics Model (Carslaw et al., 1995), and from the liquid drop model. The thermodynamic data for intermediate size particles are a smooth interpolation of the data from these sources. An exponential form of the correction to the liquid drop model Gibbs free energy for neutral cluster as introduced by Lovejoy et al. (2004) is used. In the present case, the exponential parameters have been adjusted slightly to better match the measured dimer and trimer data, and the correction reads $3e^{-(m+n)/5}$ kcal/mol for the addition of a sulfuric acid molecule to a $(H_2SO_4)_{m-1}(H_2O)_n$ and for the addition of a water molecule to a $(H_2SO_4)_m(H_2O)_{n-1}$ cluster. The present neutral thermodynamic data predict more stable small neutral clusters and more efficient neutral nucleation than the previous treatment (Lovejoy et al., 2004).

The rate coefficients for sulfuric acid uptake and loss by the aerosol particles, for the coagulation of the aerosol particles among themselves and with cirrus ice crystals, and for the recombination of the negatively charged aerosol with cations are averaged over the equilibrium H_2O content probability distribution of the aerosol. This simplification holds well in the troposphere, where water is more abundant by orders of magnitude than sulfuric acid, so that the clusters always have enough time to equilibrate with respect to water uptake/loss before colliding with a H_2SO_4 molecule. Details of the rate coefficient calculations are given by Lovejoy et al. (2004). A mass accommodation coefficient of 1 is assumed for the loss of gas phase sulfuric acid and aerosol particles onto cirrus ice crystals based on the work of Hanson (2005), and the corresponding rate coefficients are calculated with the expression of Fuchs (1964), which gives Brownian diffusion rate coefficients for loss onto particles much larger than the air mean free path. In the rate coefficient calculation the cirrus particles are represented by spheres with the surface area and mass of hexagonal column ice crystals with an aspect ratio of 3.

The model implements a hybrid kinetic-sectional scheme: in the kinetic part, the model resolves the concentrations of the $(H_2SO_4)_i(H_2O)_{j(i)}$ and $HSO_4^-(H_2SO_4)_{i-1}(H_2O)_{j^-(i)}$ clusters individually with $i \leq 21$. $j(i)$ and $j^-(i)$ are the most probable H_2O contents of the clusters based on the the cluster water content probability distribution in equilibrium. For $i > 21$ up to particle diameters of $\sim 1\,\mu$m the model uses geometric bins. The size distribution within these bins is resolved with linear functions, which suppresses numerical diffusion better than a doubling of the bin number at a negligible computational expense. Along a trajectory, the rate coefficients and most probable cluster H_2O contents are recalculated whenever temperature or relative humidity change by more than 0.5 K or 2 percentage points, respectively, whichever occurs first. A reduction of these values has no effect on the conclusions of this work. The initial anion in the model is assumed to be $NO_3^-(HNO_3)$, the cation population is represented by $H_3O^+(H_2O)_4$.

3 Input data

We operate the model offline on trajectories in the upper troposphere near 12.5 km, generated with a detailed 1-D cirrus model (Jensen and Pfister, 2004) which describes ice crystal nucleation, deposition growth, vertical advection of ice crystals and water vapor, and ice crystal sedimentation. In this work we focus on cirrus clouds that form in either a slow (-10^{-4} K s^{-1}) or a fast (-10^{-3} K s^{-1}) updraft, resulting in larger but less numerous or smaller but more numerous ice particles, respectively: The largest ice crystal concentration on the slow updraft trajectory is 0.012 cm^{-3}, with a size distribution peak near 60 μm particle size, and 0.373 cm^{-3} on the fast trajectory, with a size distribution peak near 30 μm particle size. The average ice surface area concentration is considerably higher in the fast updraft cirrus with 407 $\mu m^2\,cm^{-3}$, versus 28 $\mu m^2\,cm^{-3}$ in the slow updraft cirrus. These surface area concentrations are calculated assuming that the cirrus ice crystals are hexagonal columns with an aspect ratio of 3, and the particle sizes are diameters of volume-equivalent spheres.

Figure 1 shows the evolution of pressure, temperature, RH, and ice surface area concentration along the two trajectories. The irregular structure of the slow updraft cirrus ice surface area time series (Fig. 1a) is due to sedimentation of the cirrus particles from and across the considered air parcel. A similar but less prominent variability is seen in the fast updraft cirrus ice surface area time series (Fig. 1b).

The cirrus considered in this work form in the absence of convective activity, and the chemical composition and aerosol properties along the trajectories need to be specified accordingly. However, upper tropospheric chemical composition and aerosol properties exhibit a fair amount of variability due to transport of anthropogenic and volcanic emissions (Thornton et al., 1996), and due to convection, which lifts boundary layer air and initiates aerosol formation aloft, most notably in the tropics (Clarke et al., 1998; Kazil et al., 2006). The specification of a typical upper tropospheric background chemical and aerosol state is therefore not straightforward. Based on their systematic measurements of upper tropospheric aerosol concentrations, Minikin et al. (2003) give an average concentration of Aitken particles (with diameters >14 nm) of 770 cm^{-3} (at 273 K and 1000 hPa) at northern hemisphere mid-latitudes. This corresponds to 175 particles per cm^3 in the ambient conditions at the start of our trajectories. We neglect the concentrations of ultrafine aerosol measured by Minikin et al. (2003), who attribute these particles to locally or regionally confined pollution events. Hagen et al. (1995) measured concentrations of aerosol with diameters >17 nm in the mid-latitude upper troposphere. They identified two types of aerosol size distributions in and around cirrus clouds: One that can be well described with a single log-normal distribution function, and the other being characterized by elevated concentrations of small particles, possibly originating from a recent nucleation event. We therefore initialize our model with a preexisting log-normal aerosol size distribution with a geometric mean diameter of 62.5 nm and a geometric standard deviation of 1.45, in accord with the high altitude measurements of Hagen et al. (1995). The total particle concentration of this initial size distribution is 175 cm^{-3}, its surface area concentration 2.84 $\mu m^2\ cm^{-3}$.

For the calculation of the H_2SO_4 production rate, OH and SO_2 concentrations need to be specified. We assume SO_2 volume mixing ratios between 10 and 200 ppt, with a median near 40 ppt based on observations in the Pacific upper troposphere north of 20° (Thornton et al., 1999). Upper tropospheric OH mixing ratios at northern mid-latitudes range up to 0.4 ppt (Jaeglé et al., 2000). We set the noon OH mixing ratio to 0.3 ppt, corresponding to a concentration of $1.7\times10^6\ cm^{-3}$, and parameterize the OH diurnal cycle as a half sine centered around noon, with a day length of 12 h, while setting nighttime OH concentrations to zero. The production rate of sulfuric acid is then calculated under the assumption that the reaction SO_2 + OH is the rate-limiting step of the oxidation chain $SO_2 \rightarrow H_2SO_4$ (Lovejoy et al., 1996). We use solar maximum galactic cosmic ray ionization rates calculated with the code of O'Brien (2005) for 210° E, 35° N and for the ambient conditions along the trajectories.

4 Results

4.1 Daytime cirrus

Figure 2 shows gas phase H_2SO_4 and aerosol concentrations calculated with our aerosol parcel model on the slow (Fig. 1a) and on the fast (Fig. 1b) updraft trajectory for different SO_2 volume mixing ratios. The cirrus formation has been synchronized with sunrise in order to examine the effect of cirrus particles on in-cloud aerosol formation.

Within the slow updraft cirrus (Fig. 2a), gas phase H_2SO_4 concentrations rise to levels permitting aerosol nucleation at SO_2 mixing ratios as low as 15 ppt, yielding several hundred supercritical particles per cm^3. At 45 ppt SO_2, many thousand supercritical particles form per cm^3 in the cloud, but only negligible concentrations of particles larger than 3 nm in diameter. These larger particles appear at 60 ppt SO_2, and attain appreciable concentrations of several thousand per cm^3 within the cloud at 90 ppt SO_2.

In the fast updraft cirrus the large surface area concentrations remove sulfuric acid quickly from the gas phase (Fig. 2b). This rapid removal manifests most prominently as dents in the H_2SO_4 concentration that are collocated with peaks in the surface area time series. Nucleation is strongly inhibited and supercritical aerosol concentrations remain low even at high SO_2 mixing ratios until sedimentation of the ice crystals has depleted the cloud. The dissipation of the cloud prompts an increase in H_2SO_4 concentration and aerosol nucleation, followed by the formation of larger (>3 nm diameter) particles.

4.2 Nighttime cirrus

Figure 3 shows gas phase H_2SO_4 and aerosol concentrations on the slow (Fig. 1a) and fast (Fig. 1b) updraft trajectories which have been shifted with respect to the diurnal cycle so that the cirrus clouds form at sunset, illustrating the effect of ice surface area on aerosol that formed prior to the cloud.

Aerosol particles exceeding 3 nm in diameter that formed in the course of the day endure the slow updraft cirrus cloud nearly unscathed (Fig. 3a), their slow decline is mainly due to coagulation among themselves. Particle concentrations are reduced more distinctly in the fast updraft cirrus (Fig. 3b), but a fair portion of the 3 nm particles survives the cloud phase. The fast updraft cirrus almost instantly removes all sulfuric acid from the gas phase, while the removal is more gradual in the slow updraft case.

A closer inspection of Fig. 3 reveals that the concentration of particles larger than 3 nm is slightly higher at the time of the cirrus formation on the fast updraft trajectory (Fig. 3b) compared with the slow updraft trajectory (Fig. 3a): While the SO_2 mixing ratios are held constant along the trajectories, the SO_2 concentrations decrease due to the expansion of the air parcel in the updraft, which starts at 11:00 h (trajectory time) on the slow updraft trajectory (Fig. 1a), but at 22:30 h (trajectory time) on the fast updraft trajectory. As a consequence the SO_2 concentration is lower during daytime on the slow updraft trajectory, resulting in lower H_2SO_4 production rates.

5 Discussion

The removal of condensable gases from the gas phase is diffusion limited for particles that are much larger than the mean free path length of air, which is typically <1 μm in the troposphere. Hence cirrus ice crystals remove H_2SO_4 molecules from the gas phase less efficiently per unit surface area than smaller aerosol particles.

This is illustrated in Fig. 4, which shows the effect of variations in preexisting aerosol surface area concentration on aerosol formation in the case of the slow updraft cirrus. Three initial aerosol populations are compared, with surface area concentrations of 1.42, 2.84, and 5.68 $\mu m^2\,cm^{-3}$, corresponding to H_2SO_4 condensational sinks of 7.5×10^{-5}, 1.5×10^{-4}, and $3\times10^{-4}\,s^{-1}$, respectively. A geometric mean diameter of 62.5 nm and a geometric standard deviation of 1.45, and a SO_2 volume mixing ratio of 90 ppt is assumed in all three cases. A doubling of the preexisting aerosol surface area concentration to 5.68 $\mu m^2\,cm^{-3}$ completely halts the formation of >3 nm diameter particles, while a halving of the preexisting aerosol surface area concentration to 1.42 $\mu m^2\,cm^{-3}$ markedly boosts the concentrations of these particles (Fig. 4). The strong dependence of particle formation on preexisting aerosol surface area concentration is due to the comparably low average H_2SO_4 condensational sink of $5.3\times10^{-5}\,s^{-1}$ of the cirrus ice particles. This diffusion limited removal of sulfuric acid from the gas phase by cirrus ice, together with the low temperatures in the upper troposphere explains why aerosol formation can proceed in cirrus clouds.

Our study does not directly address anvil cirrus clouds with very large ice surface area concentrations, in which Lee et al. (2004) observed high numbers of ultrafine

ACPD
6, 12179–12197, 2006

EGU

particles: Anvil cirrus form in a highly dynamic environment associated with convection, and cannot be easily compared with the cirrus in our simulations. Nonetheless, we can explore the conditions under which aerosol formation proceeds in the presence of very large ice surface area concentrations:

Figure 5 shows results for two idealized cirrus clouds consisting of 19 μm or 78 μm ice crystals, with a surface area concentration of 1250 μm^2 cm^{-3} in both cases, and a zero preexisting aerosol surface area concentration. For 1 ppb SO_2, the cloud with the smaller crystals completely suppresses the formation of >3 nm diameter aerosol, while a massive nucleation event occurs in the cloud with the larger crystals, leading to the formation of >3 nm diameter particles at concentrations in the thousands per cm^3. The striking difference is due to the slower removal of sulfuric acid from the gas phase in the cloud with the larger ice crystals: The H_2SO_4 condensational sink is 2.2×10^{-4} s^{-1} in the case of the larger, and 8.7×10^{-4} s^{-1} in the case of the smaller ice crystals.

While not common, SO_2 mixing ratios in the ppb range have been observed in the upper troposphere (Arnold et al., 1997). A process that could establish such high SO_2 levels is the convective lifting of polluted boundary layer air which may contain SO_2 at mixing ratios of many ppb (e.g. Hanke et al., 2003). This is a plausible scenario as anvil cirrus form due to strong convective updrafts, which are capable of lifting boundary layer air as high as into the stratosphere, even at mid-latitudes (Fischer et al., 2003). Boundary layer air may also contain aerosol precursor gases other than SO_2. These precursor gases need not necessarily nucleate, but could contribute to the condensational growth of freshly nucleated sulfuric acid/water particles.

In the cases considered in our simulations, ionization rates amount to values around 30 cm^{-3} s^{-1}, but neutral nucleation dominates over charged nucleation by at least a factor of two. The charged nucleation rate may be underestimated in our model for different reasons: The cation population is represented by a proton hydrate in our model. However, positive sulfuric acid/water clusters, while less potent to promote aerosol nucleation compared with their negative counterparts at temperatures of the lower troposphere (Froyd and Lovejoy, 2003a), might grow to stable sizes in upper tropospheric conditions and thus contribute to aerosol formation. Stable neutral aerosol particles can also form from the recombination of subcritical positive and negative sulfuric acid/water clusters or other complex cations and anions.

6 Conclusions

The formation of sulfate aerosol from the gas phase in cirrus clouds is possible, and facilitated by the relatively inefficient, diffusion limited removal of sulfuric acid from the gas phase by cirrus ice crystals, and by the low temperatures in the upper troposphere. Neutral nucleation dominates over charged nucleation in our simulations. In non-convective cirrus that form in slow updrafts and thus exhibit comparably low surface area concentrations, aerosol nucleation is possible at SO_2 mixing ratios as low as 15 ppt. Formation of larger (>3 nm diameter) aerosol particles within these clouds requires SO_2 mixing ratios elevated within the range of values found in the northern mid-latitude upper troposphere. In cirrus with large area concentrations, such as formed by fast updrafts or due to convective activity, aerosol nucleation and growth are strongly inhibited, and require very high SO_2 levels to proceed. In the case of anvil cirrus, such high SO_2 concentrations could be established by transport of polluted boundary layer air into the upper troposphere, along with other aerosol precursor gases by the convective updraft that is responsible for the formation of the cirrus cloud. Aerosol particles that nucleate and grow to larger sizes before the formation of a cirrus cloud can persist in considerable numbers within the cloud, even at high ice surface area concentrations.

The concentrations of aerosol precursor gases required for aerosol nucleation within cirrus depend not only on the cirrus ice surface area concentration, but strongly on the surface area concentration of preexisting aerosol, and on the size of the cirrus ice crystals. Comparably moderate variations in preexisting aerosol surface area or ice crystal sizes can make the difference between an absent and a vigorous aerosol nucleation event.

Our simulations do not account for positive sulfuric acid/water clusters, other complex

ACPD
6, 12179–12197, 2006

cations and anions, aerosol precursor molecules other than H_2SO_4 and H_2O, or for processes such as heterogeneous chemistry on ice surfaces. While not a prerequisite, they could promote aerosol formation and growth within cirrus clouds with very high ice surface area concentrations, or when SO_2 and OH concentrations alone would not suffice.

Acknowledgements. We would like to thank D. M. Murphy (NOAA Earth System Research Laboratory) for helpful discussions. This work is supported by the National Research Council and by the NOAA Climate and Global Change Program.

References

Arnold, F., Schneider, J., Gollinger, K., Schlager, H., Schulte, P., Hagen, D. E., Whitefield, P. D., and Velthoven, P. v.: Observation of upper tropospheric sulfur dioxide- and acetone-pollution: Potential implications for hydroxyl radical and aerosol formation, Geophys. Res. Lett., 24, 57–60, doi:10.1029/96GL03693, 1997. 12188

Brock, C. A., Hamill, P., Wilson, J. C., Jonsson, H. H., and Chan, K. R.: Particle formation in the upper tropical troposphere: a source of nuclei for the stratospheric aerosol, Science, 270, 1650–1653, 1995. 12181

Carslaw, K. S., Clegg, S. L., and Brimblecombe, P.: A thermodynamic model of the system HCl-HNO_3-H2SO_4-H_2O, including solubilities of HBr, from <200 K to 328 K, J. Phys. Chem., 99, 11 557–11 574, 1995. 12182

Clarke, A. D., Varner, J. L., Eisele, F., Mauldin, R. L., Tanner, D., and Litchy, M.: Particle production in the remote marine tropospere: Cloud outflow and subsidence during ACE 1, J. Geophys. Res., 103, 16 397–16 409, 1998. 12181, 12184

Eichkorn, S., Wilhelm, S., Aufmhoff, H., Wohlfrom, K. H., and Arnold, F.: Cosmic ray-induced aerosol-formation: First observational evidence from aircraft-based ion mass spectrometer measurements in the upper troposphere, Geophys. Res. Lett., 29(14), 1698, doi:10.1029/2002GL015044, 2002. 12181

Fischer, H., de Reus, M., Traub, M., Williams, J., Lelieveld, J., de Gouw, J., Warneke, C., Schlager, H., Minikin, A., Scheele, R., and Siegmund, P.: Deep convective injection of boundary layer air into the lowermost stratosphere at midlatitudes, Atmos. Chem. Phys., 3, 739–745, 2003. 12188

Froyd, K. D. and Lovejoy, E. R.: Experimental Thermodynamics of Cluster Ions Composed of H_2SO_4 and H_2O. 1. Positive Ions, J. Phys. Chem. A, 107, 9800–9811, 2003a. 12188

Froyd, K. D. and Lovejoy, E. R.: Experimental Thermodynamics of Cluster Ions Composed of H_2SO_4 and H_2O. 2. Measurements and ab Initio Structures of Negative Ions, J. Phys. Chem. A, 107, 9812–9824, 2003b. 12182

Fuchs, N. A.: The Mechanics of Aerosols, Macmillan, 1964. 12183

Hagen, D. E., Podzimek, J., and Trueblood, M. B.: Upper-tropospheric aerosol sampled during project FIRE IFO II, J. Atmos. Sci., 52, 4196–4209, 1995. 12184, 12185

Hanke, M., Umann, B., Uecker, J., Arnold, F., and Bunz, H.: Atmospheric measurements of gas-phase HNO_3 and SO_2 using chemical ionization mass spectrometry during the MINATROC field campaign 2000 on Monte Cimone, Atmos. Chem. Phys., 3, 417–436, 2003. 12188

Hanson, D. R.: Mass accommodation of H_2SO_4 and CH_3SO_3H on water-sulfuric acid solutions from 6% to 97% RH, J. Phys. Chem. A, 109, 6919–6927, doi:10.1021/jp0510443, 2005. 12183

Hanson, D. R. and Lovejoy, E. R.: Measurement of the thermodynamics of the hydrated dimer and trimer of sulfuric acid, J. Phys. Chem. A, 110, 9525–9528, doi:10.1021/jp062844w, 2006. 12182

Jaeglé, L., Jacob, D. J., Brune, W. H., Faloona, I., Tan, D., Heikes, B. G., Kondo, Y., Sachse, G. W., Anderson, B., Gregory, G. L., Singh, H. B., Pueschel, R., Ferry, G., Blake, D. R., and Shetter, R. E.: Photochemistry of HO_x in the upper troposphere at northern midlatitudes, J. Geophys. Res., 105, 3877–3892, doi:10.1029/1999JD901016, 2000. 12185

Jensen, E. and Pfister, L.: Transport and freeze-drying in the tropical tropopause layer, J. Geophys. Res., 109, D02207, doi:10.1029/2003JD004022, 2004. 12183, 12193

Kazil, J., Lovejoy, E. R., Barth, M. C., and O'Brien, K.: Aerosol nucleation over oceans and the role of galactic cosmic rays, Atmos. Chem. Phys., 6, 4905–4924, 2006. 12181, 12184

Kulmala, M., Reissell, A., Sipilä, M., Bonn, B., Ruuskanen, T. M., Lehtinen, K. E. J., Kerminen, V.-M., and Ström, J.: Deep convective clouds as aerosol production engines: Role of insoluble organics, J. Geophys. Res. (Atmos.), 111, 17202, doi:10.1029/2005JD006963, 2006. 12181

Lee, S.-H., Reeves, J. M., Wilson, J. C., Hunton, D. E., Viggiano, A. A., Miller, T. M., Ballenthin, J. O., and Lait, L. R.: Particle Formation by Ion Nucleation in the Upper Troposphere and Lower Stratosphere, Science, 301, 1886–1889, 2003. 12181

Lee, S.-H., Wilson, J. C., Baumgardner, D., Herman, R. L., Weinstock, E. M., LaFleur, B. G., Kok, G., Anderson, B., Lawson, P., Baker, B., Strawa, A., Pittman, J. V., Reeves, J. M., and Bui, T. P.: New particle formation observed in the tropical/subtropical cirrus clouds, J. Geophys. Res., 109, 20209, doi:10.1029/2004JD005033, 2004. 12180, 12181, 12187

Liou, K.-N.: Influence of Cirrus Clouds on Weather and Climate Processes: A Global Perspective, Mon. Weather Rev., 114, 1167–1199, doi:10.1175/1520-0493, 1986. 12181

Lovejoy, E. R., Hanson, D. R., and Huey, L. G.: Kinetics and products of the gas-phase reaction of SO_3 with water, J. Phys. Chem., 100, 19 911–19 916, doi:10.1021/jp962414d, 1996. 12185

Lovejoy, E. R., Curtius, J., and Froyd, K. D.: Atmospheric ion-induced nucleation of sulfuric acid and water, J. Geophys. Res., 109, D08204, doi:10.1029/2003JD004460, 2004. 12182, 12183

Minikin, A., Petzold, A., Ström, J., Krejci, R., Seifert, M., van Velthoven, P., Schlager, H., and Schumann, U.: Aircraft observations of the upper tropospheric fine particle aerosol in the Northern and Southern Hemispheres at midlatitudes, Geophys. Res. Lett., 30, 1503, doi:10.1029/2002GL016458, 2003. 12184

O'Brien, K.: The theory of cosmic-ray and high-energy solar-particle transport in the atmosphere, in: The natural radiation environment VII, edited by: McLaughlin, J. P., Simopoulos, E. S., and Steinhäusler, F., Elsevier, seventh International Symposium on the Natural Radiation Environment, Rhodes, Greece, 20–24 May, 2002, 2005. 12185

Thornton, D. C., Bandy, A. R., Blomquist, B. W., Davis, D. D., and Talbot, R. W.: Sulfur dioxide as a source of condensation nuclei in the upper troposphere of the Pacific Ocean, J. Geophys. Res., 101, 1883–1890, 1996. 12184

Thornton, D. C., Bandy, A. R., Blomquist, B. W., Driedger, A. R., and Wade, T. P.: Sulfur dioxide distribution over the Pacific Ocean 1991-1996, J. Geophys. Res., 104, 5845–5854, 1999. 12185

Wang, P.-H., Minnis, P., McCormick, M. P., Kent, G. S., and Skeens, K. M.: A 6-year climatology of cloud occurrence frequency from Stratospheric Aerosol and Gas Experiment II observations (1985–1990), J. Geophys. Res., 101, 29 407–29 430, doi:10.1029/96JD01780, 1996. 12181

Wylie, D. P. and Menzel, W. P.: Eight Years of High Cloud Statistics Using HIRS., J. Climate, 12, 170–184, 1999. 12181

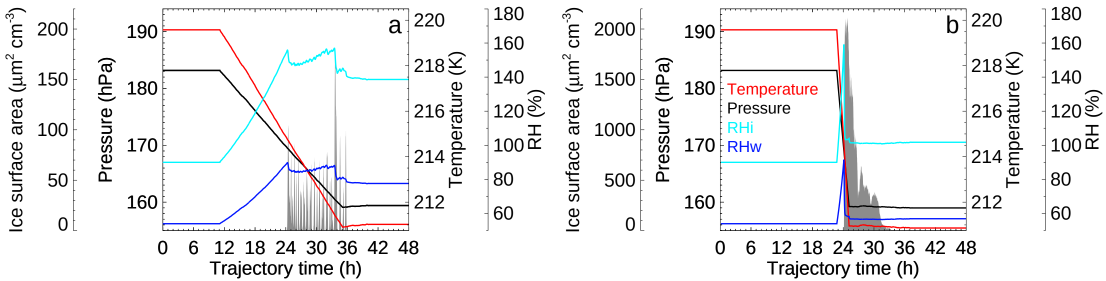

Fig. 1. Ambient conditions and cirrus ice surface area concentrations (gray areas) along the slow **(a)** and fast **(b)** updraft trajectories, generated with a 1-D cirrus model (Jensen and Pfister, 2004).

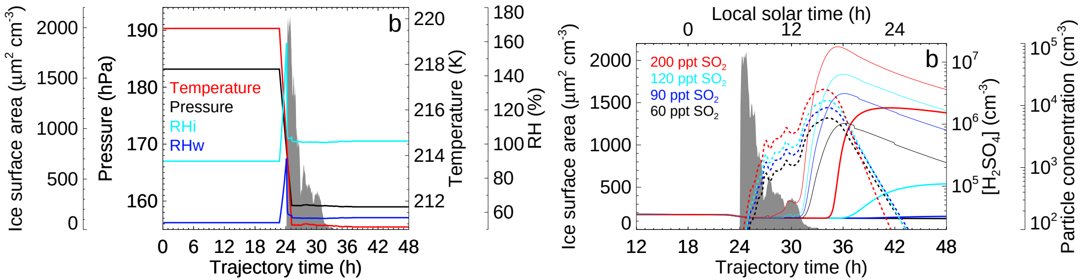

Fig. 2. Daytime slow **(a)** and fast **(b)** updraft cirrus; the cirrus ice surface area concentration is denoted by gray areas. Broken lines represent the H_2SO_4 concentration, thin solid lines the concentration of supercritical aerosol particles, thick solid lines the concentration of aerosol particles with diameters >3 nm.

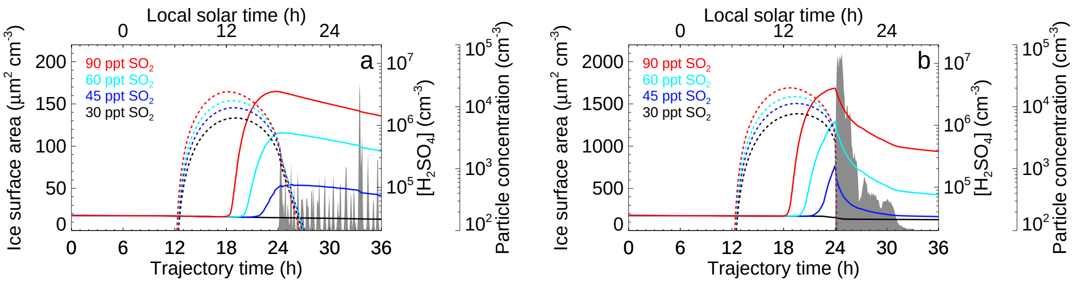

Fig. 3. Nighttime slow **(a)** and fast **(b)** updraft cirrus; the cirrus ice surface area concentration is denoted by gray areas. Broken lines represent the H_2SO_4 concentration, thick solid lines the concentration of particles with diameters >3 nm.

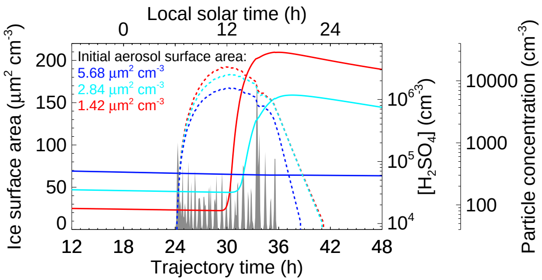

Fig. 4. Effect of preexisting aerosol surface area concentration on >3 nm aerosol particle formation in the slow updraft cirrus. Cirrus ice surface area concentration is denoted by gray areas. Broken lines represent the H_2SO_4 concentration, thick solid lines the concentration of particles with diameters >3 nm.

ACPD
6, 12179–12197, 2006

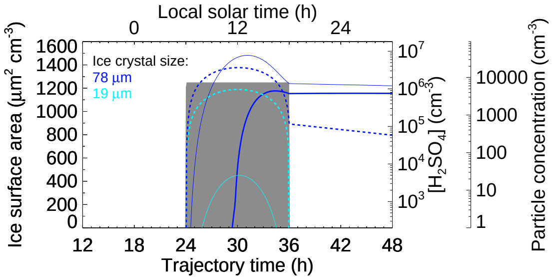

Fig. 5. Aerosol formation in two idealized cirrus clouds with an ice surface area concentration of 1250 $\mu m^2\ cm^{-3}$ (gray area), at constant conditions of 170 hPa, 210 K, and 150% relative humidity over ice. The first cloud consists of 19 μm, the second of 78 μm ice crystals. The day length is 12 h, the noon OH volume mixing ratio 0.3 ppt, and the SO_2 volume mixing ratio 1 ppb in both cases. Preexisting aerosol surface area concentration has been set to zero. Broken lines represent the H_2SO_4 concentration, thin solid lines the concentration of supercritical aerosol particles, thick solid lines the concentration of aerosol particles with diameters >3 nm. Nucleation is negligible in the presence of the smaller, but vigorous in the presence of the larger ice crystals. In the latter case, >3 nm diameter aerosol particles are produced in vast numbers.